

Positron probing of disordered regions in neutron-irradiated silicon

Nikolay Arutyunov^{*1,2,3}, Nick Bennett⁴, Neil Wight⁴, Reinhard Krause-Rehberg³, Vadim Emtsev², Nikolay Abrosimov⁵, and Vitalii Kozlovski⁶

¹ Institute of Electronics, 700170 Tashkent, Uzbekistan

² Ioffe Physico-Technical Institute, 194021 St. Petersburg, Russia

³ Department of Physics, Martin Luther University Halle, 06120 Halle, Germany

⁴ Nano-Materials Lab., School of Engineering and Physical Science, Heriot-Watt University, Edinburgh EH14 4AS, UK

⁵ Leibniz Institute for Crystal Growth, 12489 Berlin, Germany

⁶ St. Petersburg Polytechnical State University, 195251 St. Petersburg, Russia

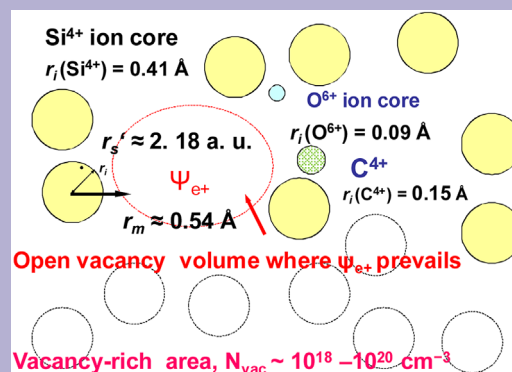
Received 27 May 2016, revised 21 September 2016, accepted 27 September 2016

Published online 21 October 2016

Keywords disordered materials, neutron irradiation, positron annihilation, silicon, vacancies

* Corresponding author: e-mail n_arutyunov@yahoo.com, Phone: +49 (0)345 552 8502, Fax: +49 (0)345 552 7158, www.researchgate.net/profile/nikolay_arutyunov

The vacancy-rich disordered regions (DR) playing a key role in improving the thermoelectric figure-of-merit of silicon thermoelectric generators by reducing (by $\sim 90\%$) the thermal conductivity, have been probed with positrons. The DR were created by irradiating n-Cz-Si(P) material with the fast reactor neutrons. The parameter of the electron density $r_s' \approx 2.18$ a.u. contacting positrons in DR has been reconstructed using the data of the angular correlation of the annihilation radiation (ACAR); the amendments to the r_s' value associated with the ion core electrons were taken into account. It is argued that the ion cores of atoms of silicon as well as the ones of the as-grown impurities (O, C) are involved in the open vacancy volume to be probed with positrons: a relaxation of the ion cores directed inward toward the vacancy volume seems to take place. These positron traps are formed beyond the vacancy-rich area of the disordered region. In the course of isochronal annealing, the traps are stable up to $T_{\text{anneal}} \approx 520^\circ\text{C}$ when a recovery of ACAR parameters begins and then it continues up to $\sim 1050^\circ\text{C}$.



A vacancy center containing positrons in the open vacancy volume beyond the vacancy-rich area of the disordered region is shown schematically. The emission of electron–positron annihilation gamma-quanta dominates from within these positron traps. The values of both the electron–positron ion core radius (r_m) and electron density (parameter r_s') suggest a relaxation directed toward inwards the open vacancy volume: the impurity atoms of oxygen and carbon are, perhaps, involved in the center.

© 2016 WILEY-VCH Verlag GmbH & Co. KGaA, Weinheim

1 Introduction It has been demonstrated recently [1, 2] that the thermal conductivity of Si thermoelectric generators may be reduced by $\sim 90\%$ by creating vacancy-rich films. As a temperature difference across the module plays a key role in the thermoelectric performance,

information about the microstructure of the open vacancy volume of defects in these films is of great importance. The vacancy-rich disordered regions (DR) created in Si by self-implantation repress the long wavelength phonon modes that contribute strongly to the thermal transport in bulk

Si [3]. An approach to create DRs that reduce Si's thermal conductivity in a similar way has been previously shown using neutron irradiation [4]. In order to gain insight into the electron and structural properties of the DRs, we have undertaken the positron probing of these defects created in silicon by irradiation with fast reactor neutrons.

Having used the technique of the angular correlation of the annihilation radiation (ACAR), we have studied the emission of gamma-quanta originating from within the open vacancy volume of defects of DR. Moreover, the high-momentum ACAR resulted from the ion cores of atoms tied to this vacancy volume has been investigated.

The data have been processed and analyzed within the framework of the most generalized approach allowing one to express the annihilation radiation parameters via the ones characterizing the electron momentum density. It is argued that the gamma-quanta of the electron–positron annihilation are emitted from within a relaxed inward open vacancy volume of the centers involved in the DR.

2 Experimental

2.1 Material For the ACAR measurements, the material grown by the Czochralski technique (n-Cz-Si[P]) was used; the carrier concentration was $n_{300K} \sim (0.5\text{--}1.0) \times 10^{15} \text{ cm}^{-3}$. The concentrations of the oxygen and carbon impurities were less than $\sim 7 \times 10^{17}$ and $\sim 2.5 \times 10^{16} \text{ cm}^{-3}$, respectively. The thickness of the samples was $\sim 0.9 \text{ mm}$ at the sizes $5 \times 15 \text{ mm}^2$. Irradiation was carried by fast reactor neutrons at $\sim 310 \text{ K}$; the thermal neutrons had been captured by the cadmium filter of $\sim 1.5 \text{ mm}$ thickness. Below we consider the material subjected to irradiation by the dose $2.0 \times 10^{18} \text{ cm}^{-2}$. The material was treated in CP-4 etching solution to eliminate near-surface damaged layer.

2.2 Measurements of ACAR spectra The deviations from collinearity of the wave vectors of the two annihilation gamma-quanta to be emitted out of the sample in almost opposite directions underlie the measurement of ACAR spectrum [5, 6]. Such deviation is proportional to the angle $\theta \cdot 10^{-3}$ radian ($\approx \theta \times 0.06^\circ$). The long-slit scheme for recording ACAR spectra has been used [5, 6]: the angle aperture for detecting the annihilation gamma-quanta was $\Delta \leq 0.45 \times 10^{-3}$ radian (the width of the slits of detectors was 2 mm and the distance between them was 4.5 m).

The magnitude of angle (θ) of registration of the annihilation gamma-quanta is known to be proportional to the component of the momentum of the electron–positron pair, $p_z/m_0c \approx \theta \times 10^{-3}$ radian $\approx \theta \times 0.06^\circ$ which is directed in parallel to the investigated crystallographic axis (m_0 is the electron mass, c is the velocity of light in vacuum; in the text we use designation p instead of p_z). The angle θ sets up the position of detectors for registering the two annihilation gamma-quanta with almost oppositely directed wave vectors, so that the angle between the slits of detectors is $180^\circ - \theta \times 0.06^\circ$. At each consequent value of θ , the number of events of two-quantum annihilation has been

accumulated during a certain period of time: the statistical error within the region of the maximum of ACAR spectra $-4 \times 10^{-3} m_0c < p < 4 \times 10^{-3} m_0c$ did not exceed 0.55–0.65%. The β^+ -isotope ^{22}Na was embedded into a thin near-surface region of the Ta substrate. The activity of the source was $\sim 25 \text{ mCi}$.

The parameters of ACAR spectra were determined after each step of the isochronal annealing of the samples in vacuum conditions $\sim 10^{-6}\text{--}10^{-5}$ Torr; the temperature step (h) and the time (t_h) of annealing at each step were $h = 30^\circ$ and $t_h = 20 \text{ min}$, respectively. The annealing was carried out within the range $\Delta T_{\text{ann}} \sim 100\text{--}1080^\circ \text{C}$.

3 Saturation of positron trapping by defects

The fast reactor neutrons are known to create the disordered regions (DR) with efficiency estimated for $\sim 0.3\text{--}1 \text{ MeV}$ neutrons as ~ 1 DR per one neutron [7]. Starting from this, the mean distance $2R_{\text{DR}}$ between DRs having concentration N_{DR} in the investigated materials is estimated to be $2R_{\text{DR}} = (3/4\pi N_{\text{DR}})^{1/3} \sim 0.99 \times 10^{-6} \text{ cm}$; this value is shorter than the positron diffusion length in the single crystal of silicon $l_+ \approx (D_+ \tau_{\text{av}})^{1/2} \approx 2.6 \times 10^{-5} \text{ cm}$ (here the positron diffusion constant is $D_+ \approx 2.8\text{--}3.1 \text{ cm}^2 \text{ s}^{-1}$, and the bulk positron annihilation lifetime $\tau_{\text{av}} \approx 217 \text{ ps}$ value is the one known for n-Cz-Si[P] material [8]).

The condition $2R_{\text{DR}} \ll l_+$ suggests that the positron trapping rate related to DRs is saturated in the investigated material. In other words, the annihilation radiation forming ACAR spectrum originates from within DRs. Moreover, the material is at the initial stage of amorphization because the mean diameter of the DRs is about 10^{-6} cm [7] and it is close to the average distance $2R_{\text{DR}}$ between DRs.

4 Thermal stability of disordered regions Thus, the saturation of the trapping rate of positrons by DRs in the investigated neutron-irradiated material allows one to consider the ACAR spectrum as a sum of the broad and narrow components:

$$I_{\text{broad}}(p)P_c^d + I_{\text{narrow}}(p)P_0^d \approx I(p), \quad (1)$$

$$P_c^c + P_0^d = 1, \quad (2)$$

where the former bears out information about the elemental specificity of the ion cores of atoms surrounding positron: see Fig. 1 and the figure in the abstract for clarity.

The contribution P_c^d is due to emission of the annihilation radiation from within, mostly, sub-valent shells of the ion cores of atoms tied to the open vacancy volume, whereas the value of P_0^d is the intensity of emission of the annihilation quanta originating in the vacancy open volume itself.

Typical ACAR spectra obtained for the neutron-irradiated material and after its isochronal annealing at the temperature step $T_{\text{ann}} = 520^\circ \text{C}$ are shown in Fig. 1. The component $I_{\text{narrow}}(p)$ is narrower than the one obtained for the non-irradiated Si [9]: this narrowing indicates lower

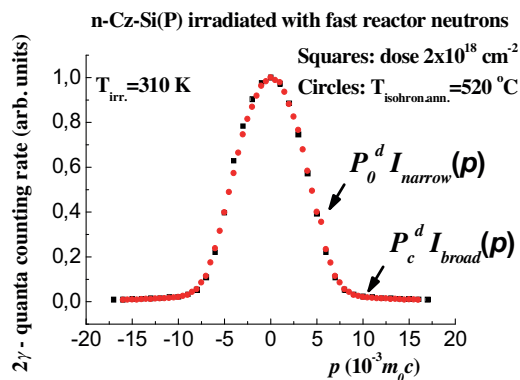


Figure 1 The ACAR spectra for the open vacancy volumes in the disordered regions (DRs) created in silicon by irradiation with the fast reactor neutrons (squares) and subjected to the isochronal annealing at $T_{\text{anneal.}} = 520\text{ °C}$ (circles). The components $P_0^d I_{\text{narrow}}(p)$ and $P_c^d I_{\text{broad}}(p)$ are the intensities of emission of the annihilation gamma-quanta from within the open vacancy volume and the ion cores of atoms involved in it, respectively; Eq. (1); see also the abstract and the schematic figure of DR there.

electron density to be probed with the positron in DR (see below). The isochronal annealing leads to disappearance of DR and the parameters of ACAR spectrum are becoming closer to the ones of non-irradiated material: it takes place at $T_{\text{ann}} \approx 1050\text{ °C}$ (these data will be discussed elsewhere).

5 Electron density beyond ion cores in disordered regions In Fig. 1, each point of the ACAR spectrum represents, approximately, a thin slice made by the detector slits through the volume of the electron–positron momentum states generating two gamma-quanta [10]. This volume is close to the spherical one as DRs are formed stochastically in the course of the neutron irradiation.

The ACAR spectrum obtained for the bonding electrons in the DR is limited by the angle which, in its turn, is proportional to the maximal momentum in the Fermi distribution of electrons, $\rho(p)$: $\theta_F \approx p_F/m_0c$. A stochastic values of $I(p)$ function are equal to the mean of the electron momentum density, $\langle \rho(p) \rangle$; further simplifications (see Refs. [6, 8] for details) result in a reciprocal parabolic function $I_{\text{narrow}}(p)$:

$$I_{\text{narrow}}(\theta) \cong \int_0^{p_F} p \rho(p) dp \approx A(p_F^2 - p^2), \quad (3)$$

where $\rho(p < p_F) \approx 1$ and $\rho(p > p_F) \approx 0$; $A \approx \text{const.}$ Having fitted function (3) to the experimental data, one can determine the “cut-off” angle of the narrow component of ACAR spectrum, namely, $\theta_F \approx p_F$.

The linearized function $P_0^d I_{\text{narrow}}(p) = I(p) - P_0^d I_{\text{broad}}(p)$ has been used for the least-squares estimate of the limiting momentum $(p_F)^2$: it ranges ~ 40.0 to $\sim 42.6 \cdot (10^{-3} m_0c)^2$ (see (Fig. 2a)). These numeral value have been obtained as a result of the positron probing of the

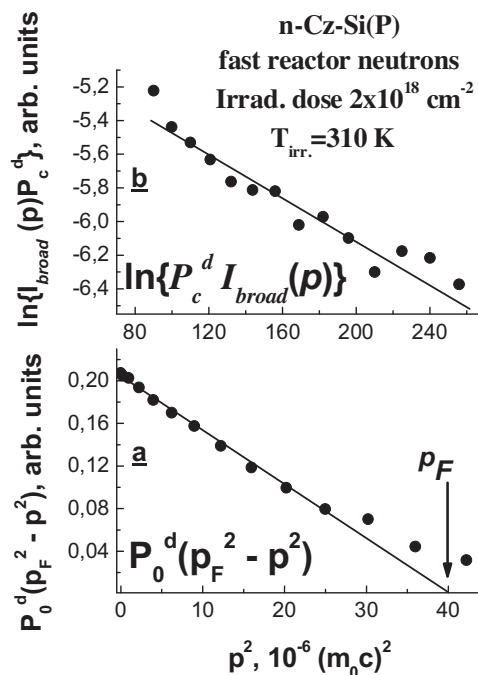


Figure 2 Linearized narrow (a; see also Eq. (3) for the interval $p < p_F$ of detected momentums of the electron–positron annihilation radiation) and high-momentum broad (b; Eq. (7), $p > p_F$) components of ACAR spectrum. The dots show the experimental data recorded for the electron–positron momentum density beyond the ion cores of atoms (a) and within them (b). The ion cores of atoms tied to the open vacancy volume of DR are schematically shown in the figure of the abstract. The arrow indicates the “cut-off” angle θ_F corresponding to the Fermi momentum $p_F \approx (39.97 \times 10^{-6})^{1/2} \approx 6.32 \times 10^{-3} m_0c$. This value characterizes the electron density around the annihilating positron beyond the ion cores of atoms. Lines are the results of the least square fitting by the functions (3) and (7). The standard errors (the correlation coefficients) were equal to 0.0001 (–0.9984) and 0.0005 (–0.9626) for the data a and b, respectively. The slope B of the upper line (b) is ~ 0.0061 (see linearized function (7) and the text in Section 6).

Fermi gas of bonding electrons whose density n' is immediately estimated via a radius r_s' of a sphere per one electron: $r_s' = (3/4\pi n')^{1/3}$.

The value of this parameter $r_s'(\text{DR}) \approx 13.99/p_F = 2.178 \pm 0.035\text{ a.u.}$ turns out to be larger by $\sim 10\text{--}11\%$ than the one obtained for non-irradiated material, $r_s'(\text{Si}) = 1.974 \pm 0.026\text{ a.u.}$ The latter value is very close to the one calculated *ab initio*: $r_s(\text{Si}) \approx 1.97\text{--}2.0\text{ a.u.}$ (see Refs. [8, 9]).

It will be noted that an amendment to r_s' value related to the electron density in the ion core region has been taken into account by subtracting the broad $P_0^d I_{\text{broad}}(p)$ component from the resulting ACAR spectrum.

The other amendment to r_s' value caused by the enhancement of the positron annihilation rate is smallest for silicon and diamond [11]. So, though the enhancement factor distorts somewhat the value of the “cut-off” angle

$\theta_F \approx p_F(r_s')$, the r_s' parameter is close to its “true” value owing to excluding the ion core electrons from consideration.

6 Annihilation gamma-quanta emitted from within ion cores of atoms in disordered regions

The positron probing of the ion cores is carried out by measuring the broad ACAR component; in Fig. 1 it is seen as a “tail” of ACAR spectrum. The ion cores play a special role in generating elementally specific annihilation radiation inasmuch as the wave functions of the electrons of the subvalent atomic shells retain their atomic character sufficiently for using them as an indicator of individual element located near the annihilation site:

$$I_{\text{broad}}(\theta) \cong \int_{p_F}^{\infty} p \rho_{\text{ion-cores}}(p) dp. \quad (4)$$

The momentum p_m may serve as a unified characteristic of the elemental specificity of the ion cores surrounding positron:

$$\theta_m \cong \int_0^{\infty} p \rho_{\text{ion-cores}}(p) dp \approx p_m/m_0c, \quad (5)$$

where $r_m \approx C(r_m)/p_m$ is a certain distance of a maximal overlapping of the positron and electron wave functions in the ion core at the moment of annihilation. The function $C(r_m)$ is, mainly, predestined by the electron states of the subvalent ion core electron shells, and for estimates of r_m values a valid assumption that $C(r_m) \approx \text{const}$ is used [12].

Averaged over a mass ion core electron states, the electron–positron radius r_m has been reconstructed for the ion cores tied to the open vacancy volume in DRs: the ACAR distribution $I_{\text{broad}}(p) \cdot P_c$ which is considered to be the normal one if it fits into Gaussian-like function has been used:

$$I_{\text{broad}}(p)P_c^d \approx P_c^d I_c^d(q, r_m) \approx L(q, r_m) \exp(-q^2), \quad (6)$$

$$y = \ln\{I_{\text{broad}}(p)P_c^d\} = A - Bx, \quad (7)$$

where $q = C(r_m)^{1/2}\theta$, $C(r_m) \approx \text{const}$, and $L(q, r_m)$ is slowly varying function in comparison with the one of $\exp(-q^2)$.

The linearized function (7) fits reliably into experimental data ranging from $p \approx 10 \times 10^{-3} m_0c$ to $\geq 17 \times 10^{-3} m_0c$ (see Fig. 2b): $x = p^2$, $A = \ln\{L(q, r_m)\}$, and $B = 1/C(r_m)$.

The r_m (DR) value proves to be equal to $\sim 0.539 \pm 0.004 \text{ \AA}$ which is somewhat shorter (by $\sim 17\text{--}19\%$) than the one for the material of reference (i.e., for non-irradiated n-Cz-Si[P] crystal, where $r_m(\text{Si})$ values are $\approx 0.6\text{--}0.64 \text{ \AA}$ [9]).

Having integrated the fitted function (6) over the range of $\sim (0\text{--}17 \times 10^{-3} m_0c)$, we immediately obtain $P_c^d(\text{DR}) \sim 7.8\text{--}8\%$ whose value is somewhat smaller than the one for the non-irradiated material, $P_c^d(\text{Si}) \sim 10\text{--}11\%$. The inequalities $r_m(\text{DR}) < r_m(\text{Si})$ and $P_c^d(\text{DR}) < P_c^d(\text{Si})$ are a salient evidence for a marked effect of the relaxation of the ion cores of atoms tied to the open vacancy volume. It is this relaxation that contributes to the electron density in the open vacancy volume resulting in the numeral value $r_s'(\text{DR}) \approx 2.178 \pm 0.035 \text{ a.u.}$ which is by $\sim 10\%$ larger than the one for non-radiated material, $r_s'(\text{Si}) = 1.974 \pm 0.026 \text{ a.u.}$

One can not exclude an involvement of the atoms of residual impurities such as oxygen and carbon in the microstructure the center shown schematically above, in the abstract. In this case, the positron is probing the electron states of bonding which have an ion-covalent character with a quite large ionicity. A higher energy of such bonding contributes to the thermal stability of DR influencing the heat transport. There is good reason to believe that the availability of the high concentration of low-energetic phonons with $E_{\text{ph}} \ll k_B T$ underlies the cascade phonon-assisted positron trapping into the localized states at the vacancy centers under consideration.

7 Conclusions The parameter of the electron density contacting the positron in the open vacancy volume in DR is equal to the value $r_s'(\text{DR}) = 2.178 \pm 0.035 \text{ a.u.}$ which by $\sim 10.3\%$ larger than the one obtained by ACAR for the material of reference, $r_s'(\text{Si}) = 1.974 \pm 0.026 \text{ a.u.}$ Being shorter by $\approx 17\text{--}19\%$ in comparison with the value for initial non-irradiated material, the electron–positron ion radius $r_m(\text{DR}) = 0.539 \pm 0.004 \text{ \AA}$ indicates a relaxation of the ion cores directed inward toward the open vacancy volume.

Involvement of the oxygen/carbon impurity atoms contributing to the relaxation shifts seems to take place beyond the vacancy-rich area of DR. It is these DRs in the neutron-irradiated material that contribute greatly to improving the figure-of-merit of silicon thermoelectric generators.

The open vacancy volume is thermally stable in the course of isochronal annealing up to $T_{\text{anneal.}} = 520^\circ\text{C}$; then the recovery of the crystal structure of silicon begins and it continues up to $T_{\text{anneal.}} \sim 1050^\circ\text{C}$.

References

- [1] N. S. Bennett, N. M. Wight, S. R. Popuri, and J. W. G. Bos, *Nano Energy* **16**, 350 (2015).
- [2] N. M. Wight and N. S. Bennett, *Solid State Phenom.* **242**, 344 (2016).
- [3] S. K. Estreicher, T. M. Gibbons, M. B. Bebek, and A. L. Cardona, *Solid State Phenom.* **242**, 335 (2016).
- [4] H. J. Albany and M. Vandevyver, *J. Appl. Phys.* **38**, 425 (1967).
- [5] N. Yu. Arutyunov and V. V. Emtsev, *Mater. Sci. Semicond. Process.* **9**, 788 (2006).

- [6] N. Yu. Arutyunov, in: *Condensed Matter – New Research*, edited by M. P. Das (Nova Science, New York, 2007), chap. 7.
- [7] V. S. Vavilov, *The Influence of Irradiations on Semiconductors* (Fizmatgiz, Moscow, 1963), pp. 196–202 (in Russian); see also, e.g., L. J. Cheng and J. Lori, *Phys. Rev.* **171**, 856 (1968); S. Ghosh and G. Sargent, *J. Mater. Sci.* **7**, 153 (1972).
- [8] R. Krause-Rehberg and H. S. Leipner, *Positron Annihilation in Semiconductors* (Springer-Verlag, Berlin, 1999), p. 56.
- [9] N. Yu. Arutyunov and R. Krause-Rehberg, *Solid State Phenom.* **95–96**, 507 (2003).
- [10] R. Ferrel, *Rev. Mod. Phys.* **28**, 308 (1956).
- [11] B. Barbiellini, in: *New Directions in Antimatter Chemistry and Physics*, edited by C. M. Surko and F. A. Gianturco (Kluwer Academic Publishers, Netherlands, 2001), chap. 9.
- [12] L. D. Landau and E. M. Lifshits, *Quantum Mechanics: Non-Relativistic Theory* (Fizmatgiz, Moscow, 1963), p. 69 (in Russian).